RT Modelling of CMEs Using WSA-ENLIL Cone Model

A. Taktakishvili

CCMC/SWRC

NASA Goddard Space Flight Center

In this presentation we will make an introduction to the WSA-ENLIL Cone model, used at SWRC to model propagation of coronal mass ejections (CMEs) in the heliosphere.

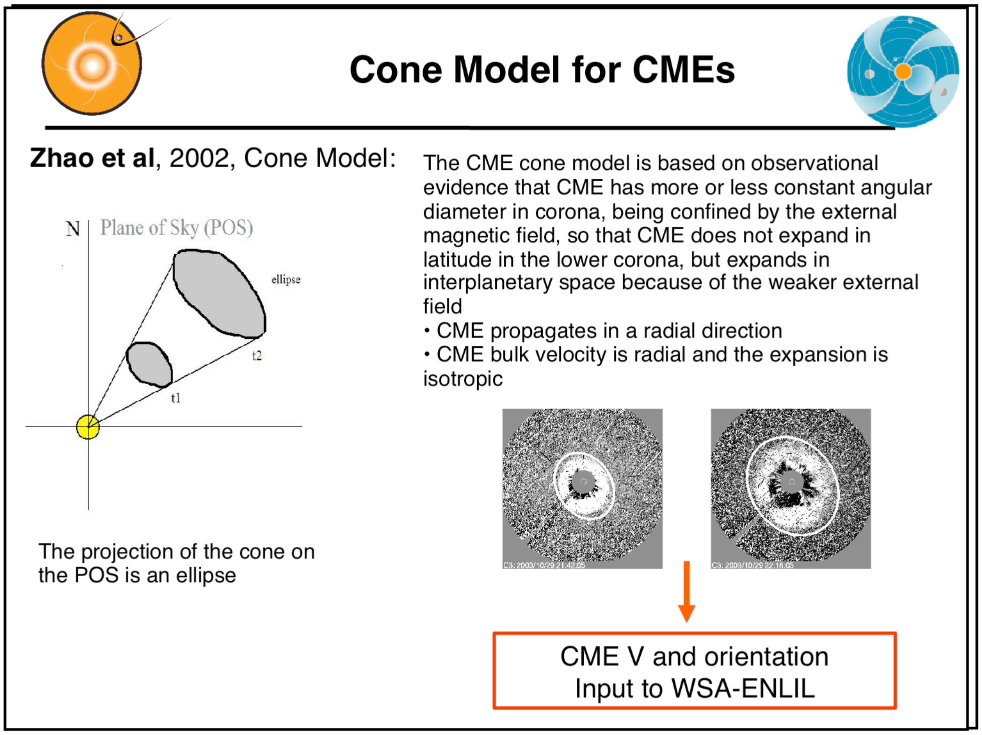

Zhao was the first to come up with the Cone model of CME. The CME cone model is based on observational evidence that CME has more or less constant angular diameter in corona, being confined by the external magnetic field, so that CME does not expand in latitude in the lower corona, but expands in interplanetary space because of the weaker external field. The assumptions are the following:

- CME propagates with nearly constant angular width in a radial direction
- CME bulk velocity is radial and the expansion is isotropic

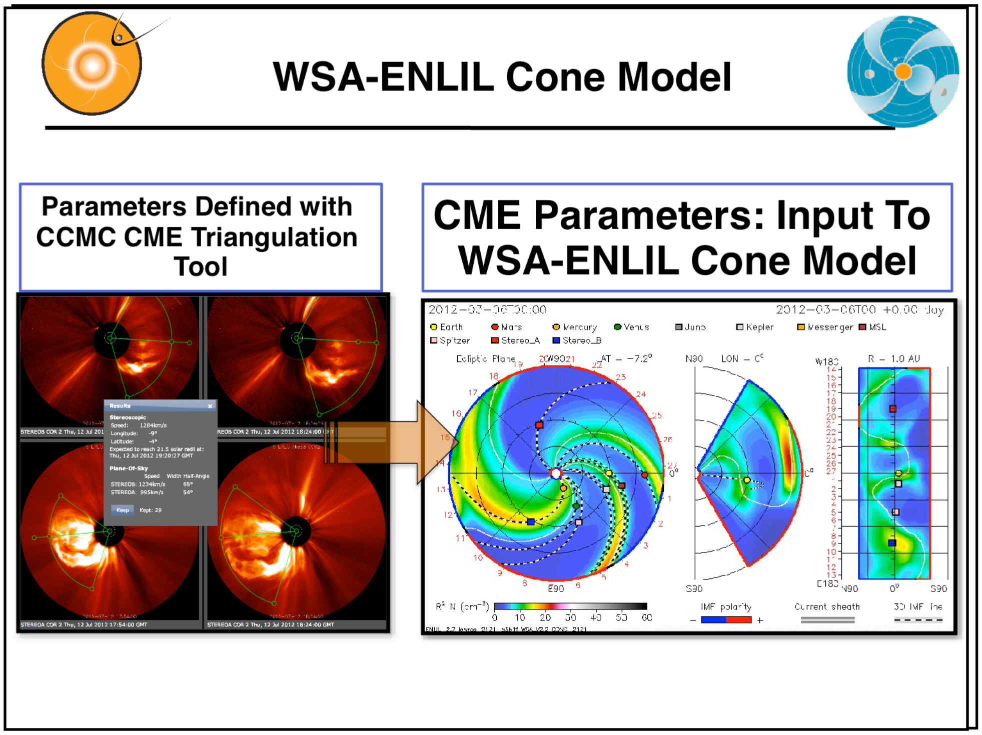

Parameters defined with CCMC CME Triangulation Tool (CAT) or other tools are used as input CMEpParameters to WSA-ENLIL Cone Model.

SWPC CME Analysis Tool

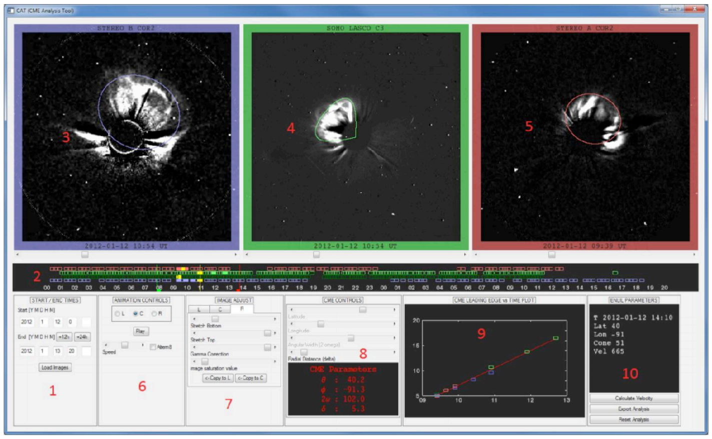

4

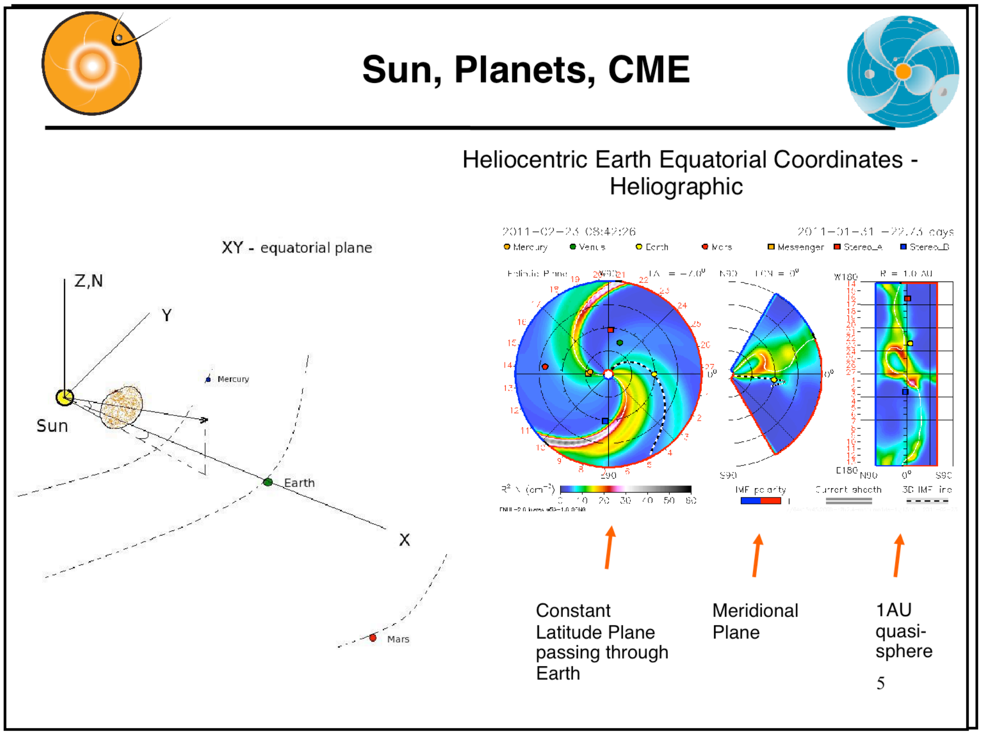

This schematic shows CME in global perspective and explains coordinate system of the WSA-ENLIL model.

XY is the equatorial plane (plane of the Sun equator). Z axis points to to north pole of the Sun. Earth is located in the ecliptic plane, which forms some variable angle with the equatorial plane (changes from -7.5 deg to 7.5 deg).

The first panel in WSA-ENLIL plot shows a plane passing through the Earth and is parallel to equatorial plane. The second panel is a meridianal cut passing through the Earth. The latitude goes from -60 to 60 degrees.
The third panel shows Longitude-Latitude map of a quasi sphere at 1 AU and with The cut off for Latitude > |60 deg| .

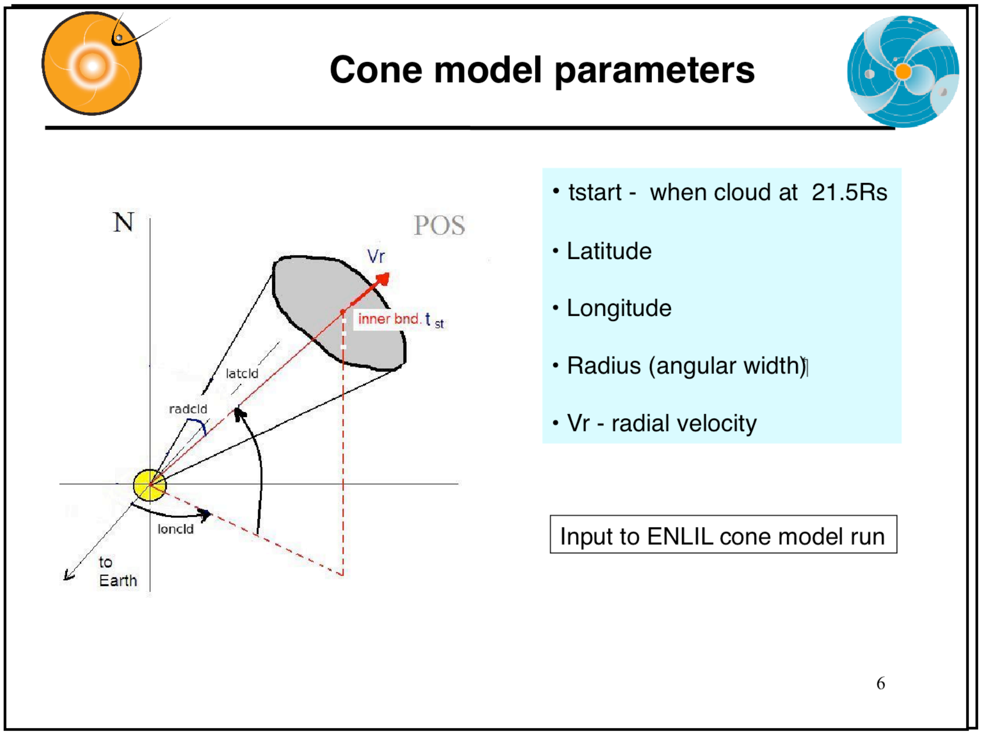

Parameters defined with CCMC CME Triangulation or other Tools yield CME Parameters: Input To WSA-ENLIL Cone Model. These parameters are:

1- start time of CME at 21.5 Rs (inner boundary of the ENLIL model)
2- Cone axis latitude
3- Cone axis longitude
5- Cone Radius – half angle of the cone angular width
6- Radial Velocity

Wang Sheely Arge model (WSA) - Input to ENLIL

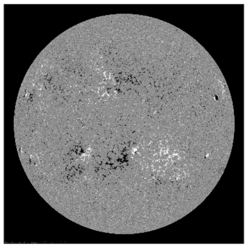

- **PFSS** (Potential Field Source Surface)**.**
  Input: synoptic map photospheric magnetogram.
  Force free (even current free) solution with radial field at 2.5 Ro.
- **Schatten Current Sheet**.
  Input: PFSS.
  Modifies the sign of radial field to positive to prevent reconnection, creates potential solution with radial boundary conditions, restores the sign in the new solution at 5 Ro.

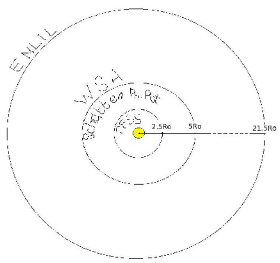

Assuming radial constant speed flow at 5 Ro uses **empirical formula for speed,** determined by the rate of divergence of the magnetic field at 5 Ro and proximity of the given field line to the coronal hole boundary. **WSA produces Br and Vr – input to ENLIL**

Wang-Sheeley-Arge model WSA (Wang-Sheeley-Arge, AFRL)

is the input model to the ENLIL at it's inner boundary of 21.5Rs.
The input to the WSA is daily magnetograms of the solar surface, that describe the magnetic field of the photosphere.

WSA model itself consists of different models

- **PFSS** (Potential Field Source Surface)**.**
  Input: synoptic map photospheric magnetogram.
  Force free (even current free) solution with radial field at 2.5 Ro.
- **Schatten Current Sheet**.
  Input: PFSS.
  Modifies the sign of radial field to positive to prevent reconnection, creates potential solution with radial boundary conditions, restores the sign in the new solution at 5 Ro.
- **WSA.**
  Input: Schatten CS.
  Assuming radial constant speed flow at 5 Ro uses empirical formula for speed, determined by the rate of divergence of the magnetic field at 5 Ro and proximity of the given field line to the coronal hole boundary.

ENLIL - Schematic Description

ENLIL – *Sumerian God of Winds and Storms*
Dusan Odstrcil, GMU & GSFC

Input: WSA (coronal maps of Br and Vr updated 4 times a day). For toroidal components at the inner boundary- Parker spiral.

ENLIL's inner radial boundary is located beyond the sonic point: the solar wind flow is supersonic in ENLIL.

Computes a time evolution of the global solar wind for the inner heliosphere, driven by corotating background structure and transient disturbances (CMEs) at it's inner radial boundary at 21.5 Ro.

Solves ideal fully ionized plasma MHD equations in 3D with two additional continuity equations: for density of transient and polarity of the radial component of B.

8

ENLIL – Sumerian God of Winds and Storms
Dusan Odstrcil, GMU & GSFC

Input: WSA (coronal maps of Br and Vr updated 4 times a day). For toroidal components at the inner boundary- Parker spiral.

ENLIL's inner radial boundary is located beyond the sonic point: the solar wind flow is supersonic in ENLIL.

Computes a time evolution of the global solar wind for the inner heliosphere, driven by corotating background structure and transient disturbances (CMEs) at it's inner radial boundary at 21.5 Ro.

Solves ideal fully ionized plasma MHD equations in 3D with two additional continuity equations: for density of transient and polarity of the radial component of B.

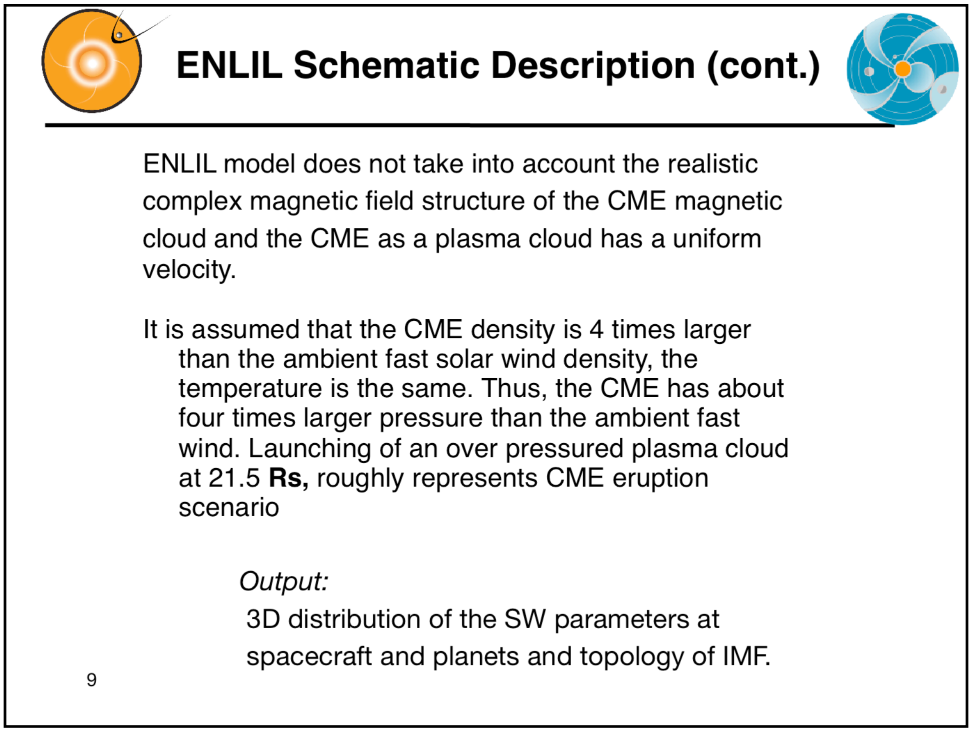

Limitation of the ENLIL model:

It does not take into account the realistic complex magnetic field structure of the CME magnetic cloud and the CME as a plasma cloud has a uniform velocity.

It is assumed that the CME density is 4 times larger than the ambient fast solar wind density, the temperature is the same. Thus, the CME has about four times larger pressure than the ambient fast wind. Launching of an over pressured plasma cloud at 21.5 **Rs,** roughly represents CME eruption scenario

Output:

3D distribution of the SW parameters at spacecrafts and planets and topology of IMF.

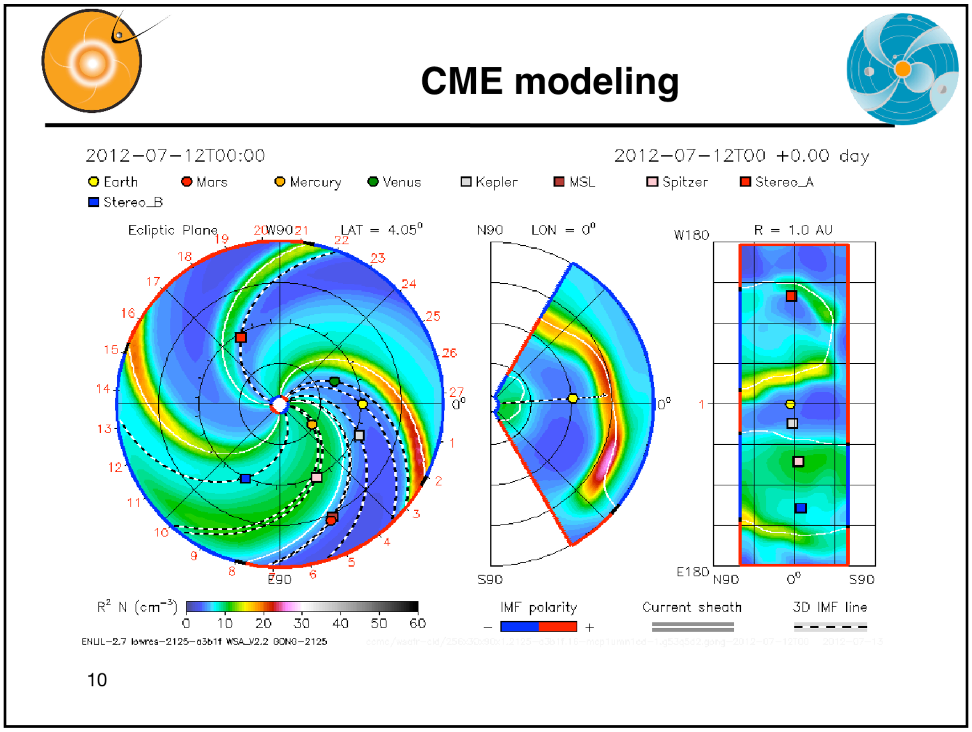

After we define the CME parameters we run the WSA-ENLIL cone model.

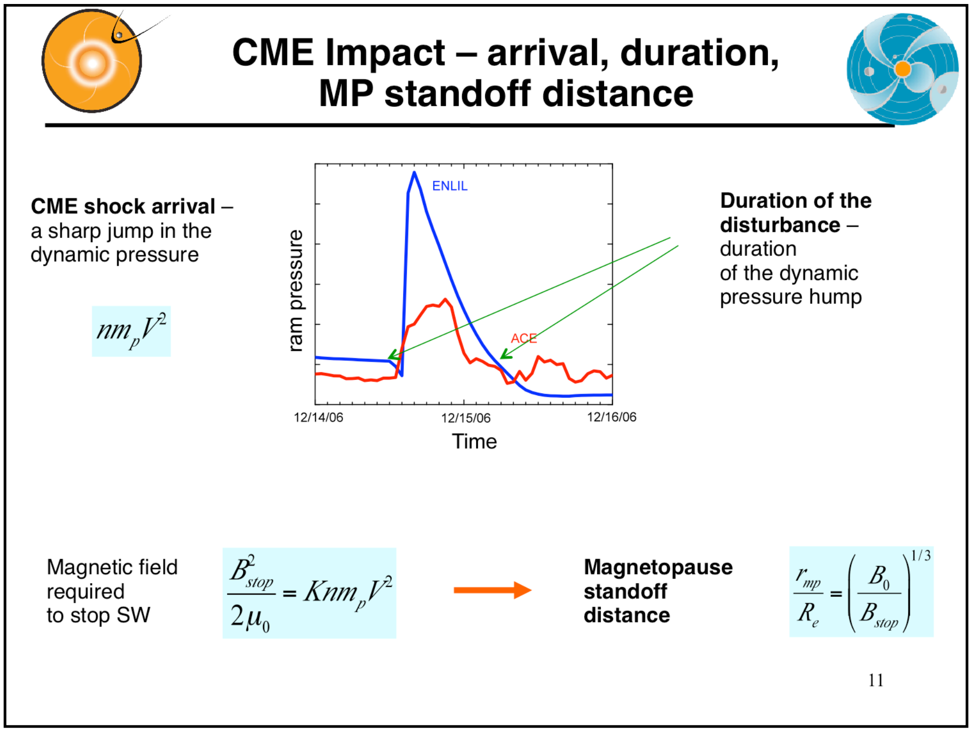

After the run is done, we estimate the CME impact on planets, satellites.

1. CME shock arrival – a sharp jump in the dynamic pressure.
2. Duration of the disturbance – duration of the dynamic pressure hump.
3. In case of the Earth we estimate also the degree of compressing of the magnetosphere: when the CME mass reaches the magnetosphere it pushes it inward and the magnetic field of the Earth is stressed like a spring to stop the CME motion.

Kp Index – P. Newel's Empirical Expression

Magnetic flux opening rate at the magnetopause

$$\frac{d\Phi_{MP}}{dt} = V^{4/3} B^{2/3} \sin^{8/3}(cl\ ang/2)$$

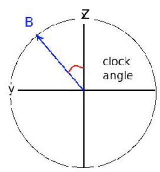

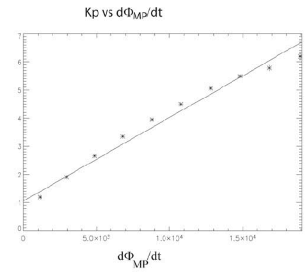

$$Kp = 9.5 - \exp\left(2.17676 - 0.000052001 \frac{d\Phi_{MP}}{dt}\right)$$

12

In case of the Earth we estimate also the Kp index – a measure of the disturbance of the magnetosphere.

We use Pat Newel's empirical formula for the Magnetic flux opening rate at the magnetopause for that and an empirical relation between Kp and d(Phi)/dt.

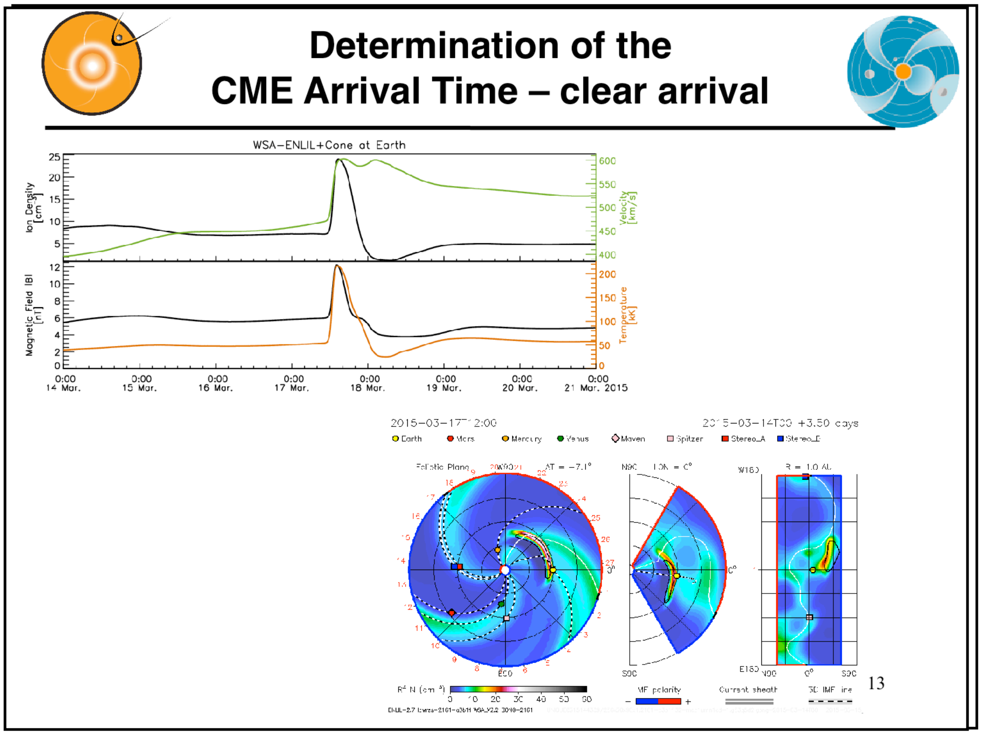

But we are not monitoring only Earth impact. Being responsible for providing space weather assessment to NASA robotic mission operators, we are monitoring possible impact of the CME on NASA missions.
So we send out another e-mail, that shows this estimate.

Determination of the CME Arrival Time from Timelines and Movies

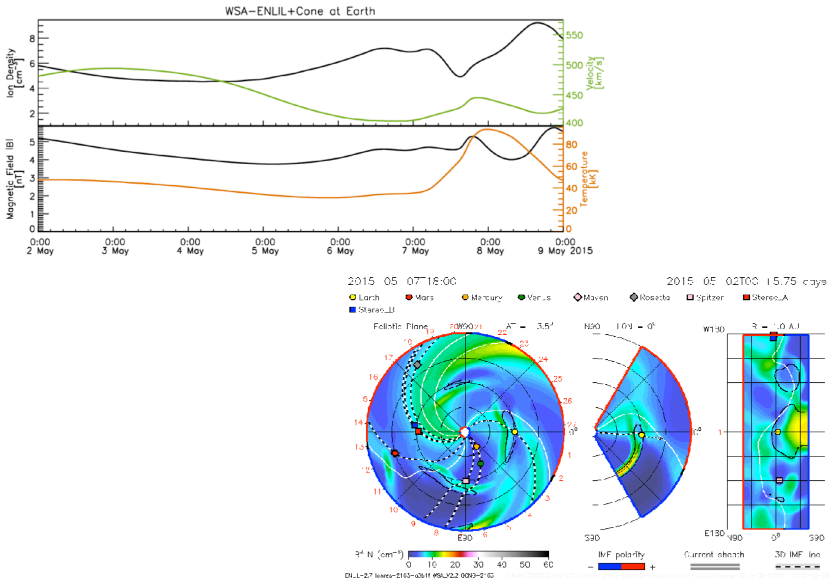

14

But we are not monitoring only Earth impact. Being responsible for providing space weather assessment to NASA robotic mission operators, we are monitoring possible impact of the CME on NASA missions.
So we send out another e-mail, that shows this estimate.

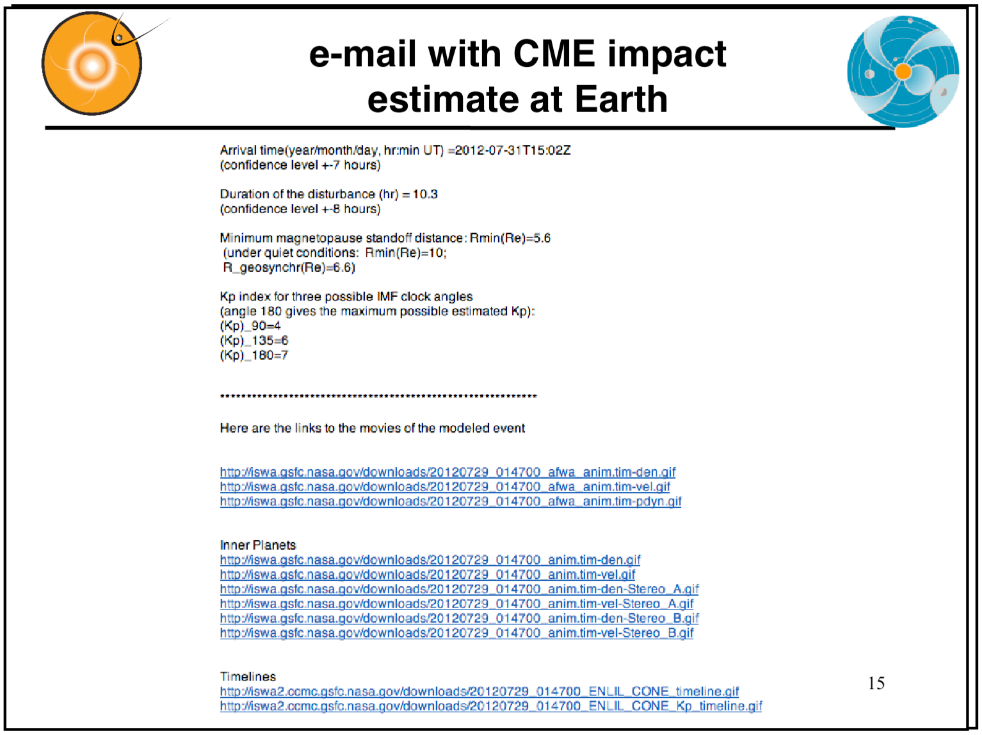

And here is our response e-mail the them in details.
It contains the CME impact estimate for the Earth
(arrival time, magnetopause standoff distance,
Kp estimate for three possible clock angles of the IMF),
and links to the modeling animation and timelines.

e-mail for NASA missions

Mars
****

CME did not hit the Mars.
or
CME impact is very weak.

****

Stereo A
****

CME did not hit the StereoA.
or
CME impact is very weak.

****

Stereo B
****
CME did not hit the StereoB.
or
CME impact is very weak.

****

Spitzer
****

Arrival time(year/month/day, hr:min UT) =2015-05-11T20:49Z

Inner Planets
http://iswa.gsfc.nasa.gov/downloads/20150509_071500_2.0_anim.tim-den.gif
http://iswa.gsfc.nasa.gov/downloads/20150509_071500_2.0_anim.tim-vel.gif
http://iswa.gsfc.nasa.gov/downloads/20150509_071500_2.0_anim.tim-den-Stereo_A.gif
http://iswa.gsfc.nasa.gov/downloads/20150509_071500_2.0_anim.tim-vel-Stereo_A.gif
http://iswa.gsfc.nasa.gov/downloads/20150509_071500_2.0_anim.tim-den-Stereo_B.gif
http://iswa.gsfc.nasa.gov/downloads/20150509_071500_2.0_anim.tim-vel-Stereo_B.gif

Inner Planet Timelines
http://iswa.gsfc.nasa.gov/downloads/20150509_071500_2.0_ENLIL_CONE_Mars_timeline.gif
http://iswa.gsfc.nasa.gov/downloads/20150509_071500_2.0_ENLIL_CONE_STA_timeline.gif
http://iswa.gsfc.nasa.gov/downloads/20150509_071500_2.0_ENLIL_CONE_STB_timeline.gif
http://iswa.gsfc.nasa.gov/downloads/20150509_071500_2.0_ENLIL_CONE_Spitz_timeline.gif
http://iswa.gsfc.nasa.gov/downloads/20150509_071500_2.0_ENLIL_CONE_Merc_timeline.gif
http://iswa.gsfc.nasa.gov/downloads/20150509_071500_2.0_ENLIL_CONE_Venus_timeline.gif

16

But we are not monitoring only Earth impact. Being responsible for providing space weather assessment to NASA robotic mission operators, we are monitoring possible impact of the CME on NASA missions. So we send out another e-mail, that shows this estimate.

Part 2:

RT Ensemble Modelling of CMEs Using WSA-ENLIL Cone Model

17

In this presentation we will make an introduction to the WSA-ENLIL Cone model, used at SWRC to model propagation of coronal mass ejections (CMEs) in the heliosphere.

Ensemble Modeling

Ensemble modeling is used in weather forecasting to quantify prediction uncertainties and determine forecast confidence

- Individual forecasts which constitute an ensemble forecast represent possible scenarios which reflects forecasting uncertainties.
- Uncertainties can be from initial conditions, observation error, and techniques and models.
- Different forecasts in the ensemble can start from different initial conditions and/or be based on different forecasting models/procedures.
- Ensemble modeling conveys the level of uncertainty in a given forecast in contrast to a categorical yes/no forecast

Ensemble Modeling with WSA-ENLIL+Cone

The current version of real-time ensemble modeling at the CCMC/SWRC evaluates the sensitivity of CME arrival time predictions from the model to initial CME parameters.

- Measure a set of *n* CME input parameters. Typically *n*=36 to 48 provides an adequate spread of input parameters, and this number can be increased as needed.

- These are used as input to an ensemble of *n* WSA-ENLIL+Cone model runs.

- This gives an ensemble of *n* profiles of MHD quantities and *n* CME arrival time predictions at locations of interest.

19

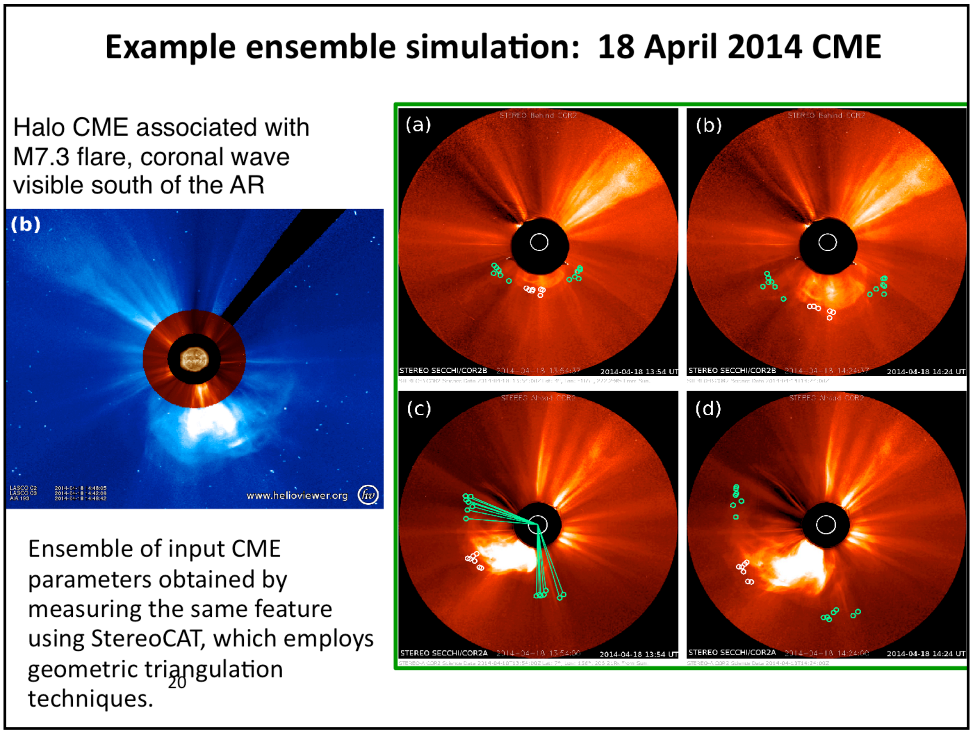

• Earth-directed partial halo CME that was first observed at 13:09 UT on 18 April 2014 by by SECCHI/COR2A. This CME was associated with an M7.3 class solar flare from Active Region 12036 located at S18°W29° with peak at 13:03 UT.

• Eruption and a coronal wave were visible south of the AR in SDO/AIA 193 Å and a nearby filament eruption was visible in AIA 304Å.

•Subsequently starting at 13:35 UT, an increase in solar energetic particle proton flux above 0.1 pfu/MeV observed by GOES Earth orbit.

Ensemble of input CME parameters obtained by measuring the same feature using StereoCAT which employs geometric triangulation techniques. The circles indicate the 6 individual leading edge (white circles near the center of the CME front) and width measurements (green circles marking the CME edges). The leading edge measurements (central circles) are later combined together to generate 6^2=36 ensemble members.

18 April 2014 CME:
WSA-ENLIL+Cone modeled magnetic field, velocity, density, and temperature profiles at Earth for 36 ensemble.

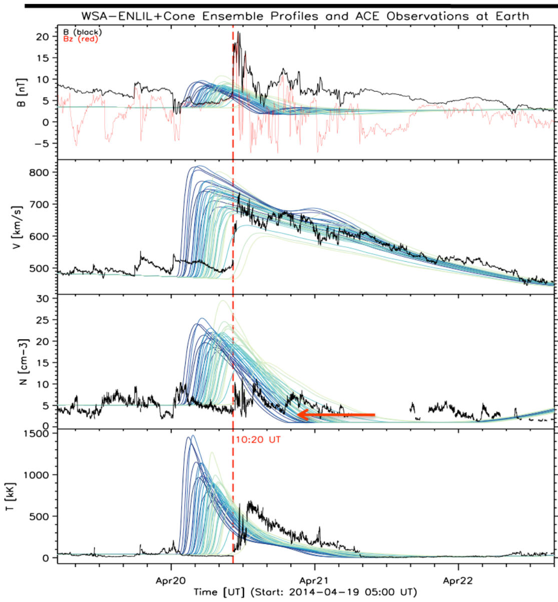

Clear ICME arrival with enhanced post-shock temperatures, enhanced magnetic field with rotations in direction, and declining solar wind speed.

18 April 2014 CME:

WSA-ENLIL+Cone modeled magnetic field, velocity, density, and temperature profiles at Earth for 36 ensemble members (traces color coded by input speed), with the observed in-situ L1 observations from ACE (black, red for Bz).

Observations show clear signatures of the arrival of an ICME, including a leading shock (abrupt increase in all the solar wind parameters at around 10:20 UT) with enhanced post-shock temperatures, enhanced magnetic field with rotations in direction, and declining solar wind speed.

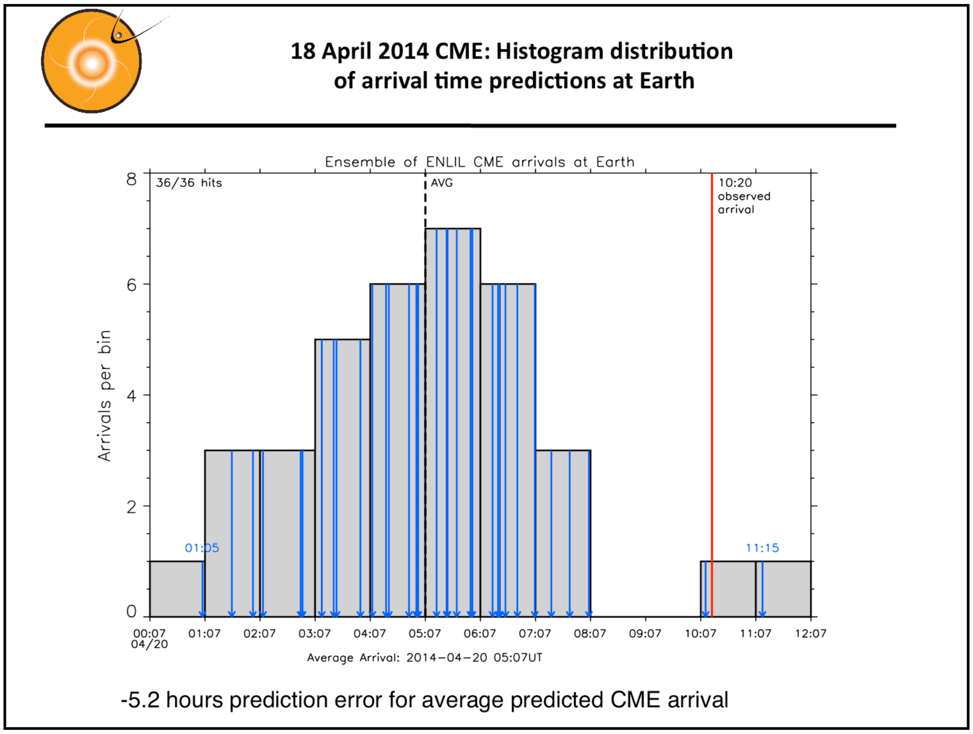

Shows a normal distribution with 50% of the predicted arrivals within one hour of the mean.

The prediction error $\Delta t_{error}=t_{predicted}-t_{observed}$ for the mean predicted CME arrival time was -5.2 hours and the observed arrival time was just within the ensemble predicted spread.